

Novel Approach to Short-Pulse and Ultra-Short Pulse Laser Ablation of Silicon Nitride Passivation Layers

Malte Schulz-Ruhtenberg*, Daniel Trusheim, Michael Smeets, Jens Holtkamp,
and Arnold Gillner

Fraunhofer Institute for Laser Technology, Steinbachstr. 15, 52074 Aachen, Germany

*malte.schulz-ruhtenberg@ilt.fraunhofer.de; phone +49 241 8906-604

ABSTRACT

Laser ablation of passivation layers is one of the most promising processes for high efficiency cell concepts in high throughput solar cell production. Especially on the front side a depth- or material-selective ablation process is required to avoid damage to the sensitive emitter. To develop a fast and reliable laser ablation process with a minimum amount of damage to the emitter it is vital to use the most suitable laser source and to optimize the processing parameters. For identification of the influence of pulse duration on cell performance after ablation a new experimental approach is chosen, where full crystalline solar cells are used as samples. In an iterative experimental sequence ablation of lines between the fingers is alternated with Suns-Voc measurements. The measurements reveal the impact of the laser ablation process on the electrical properties of the solar cell, like pseudo fill factor and open circuit voltage. The method has two decisive advantages compared to other approaches presented in earlier works: a) the preparation of special samples (e.g. full cells without front metallization) is not required and reliable commercially available standard cells can be used instead; b) the iterative nature of the approach allows an extrapolation to larger ablated areas.

Keywords: crystalline solar cells, thin film ablation, laser-induced damage, suns-voc

1. INTRODUCTION

Thin films with optical and electrical functionality play an important role in many high-tech applications: in organic LEDs and displays, solar modules and electronic circuits they are used to transport charges, modify optical properties, and emit or absorb light. Due to layer thicknesses in the range of 30 nm to a few microns very little material is required and very lightweight, thin and flexible products are possible. For crystalline silicon solar cells thin functional layers are utilized in the form of passivation and anti-reflection coatings. The former property reduces the amount of defects on the Silicon wafer surface and thus improves the lifetime of charge carriers; the latter allows a larger fraction of the sunlight to enter the solar cell. Silicon Nitride (SiN_x) layers with a thickness of 80nm are one of the most important building blocks of commercial Silicon solar cells.

Laser-based selective removal of thin functional layers is a critical step for many of the mentioned applications. As production tools, laser sources offer unique capabilities like non-contact processing, no tool-wear and a minimum of mechanical and thermal influence on the processed product due to selective and precise energy control. In thin film structuring lasers are basically used to achieve two functions: to uncover layers for contacting, or to isolate certain films from other regions. These two rather simple functions enable for example the monolithic series interconnection in thin film solar modules, which is required to reduce the current density inside the thin layers and thus ohmic losses. The challenge for laser-based structuring of thin layers is based on the requirement of a complete removal of a certain layer (or layer stack) and a minimum influence on all adjacent layers and substrates. In addition, it is often required to avoid debris on the sample, modification of the material around the area opened by laser irradiation and delamination or bulging of the processed film [1].

The local removal of SiN_x passivation layers on crystalline solar cells enables the use of modern metallization techniques, like plating or fine line printing [2, 3], and allows thinner contact lines on the solar cell of <<100 μm. It is also a possible step for high efficiency solar cell concepts [4, 5]. It has the potential to enable state-of-the-art and complex high efficiency cell concepts in high throughput photovoltaic production. In contrast to wet-chemical etching processes using etch barriers or lithographic processing, laser ablation is a one step process applicable to in-line manufacturing. Especially on the front side a selective ablation process is required to avoid damage to the sensitive emitter, because any emitter damage will lead to a higher recombination rate of the free charge carriers.

The work presented in this paper focuses on the evaluation of laser ablation of SiNx passivation layers on the front side of multi-crystalline Silicon (mc-Si) solar cells. The SiNx ablation process creates very specific requirements compared to other thin film applications due to three distinctive differences:

- highly absorbing Si substrates
- 300 nm thick highly sensitive emitter layer below the passivation layer
- textured surfaces with very high roughness

Due to the first feature, laser radiation of almost any wavelength is hardly absorbed within the thin SiNx layer, but strongly absorbed in the comparatively thick (here 200 μm) Si wafer. This results in a low modification threshold for the Silicon. The second feature shows that modification of the Si almost immediately deteriorates the electrical functionality of the solar cell. On top of this, the third feature results in an inhomogeneous intensity distribution of the incoming light on the sample surface due to scattering and reflection at the surface texture [6]. The three aspects of the material system under study illustrate the difficulties connected with the development of a damage-free laser ablation process.

This shows that the selection of the most suitable processing parameters, like wavelength and pulse duration, which result in the best electrical cell properties, is a critical development step. In this paper, a new and unique approach is chosen to achieve this goal. The approach utilizes complete commercial solar cells as test vessels, which allows reliable sample characterization. The cells are processed using a wide variety of laser sources with 355 and 532 nm wavelength and pulse durations ranging from 200 fs to 40 ns.

2. EXPERIMENTAL DETAILS

2.1 Approach

For the application in industrial production processes, laser sources offer high flexibility due to the wide range of selectable parameters. Often, each process and each material to be processed require carefully selected processing parameters and the identification of the proper laser source. The development of a laser process for solar cell manufacturing usual demands the production of hundreds or thousands of cells, before reliable data is obtained. In this paper, this difficulty is avoided by using fully processed commercial mc-Si solar cells, ablating the SiNx coating and characterizing the treated cells using a Sinton Suns-Voc station. In this way, the influence of a wide range of laser parameters used for the ablation process is evaluated in the form of degradation of electrical cell properties.

Ablation is taken out between the metal fingers on standard H-cells (details on used samples is given in section 2.2). The ablated area is framed by two neighboring fingers and the busbars. The variation of the opened area is realized by an iterated sequence of ablation and subsequent characterization. Figure 1 shows a sketch of this approach.

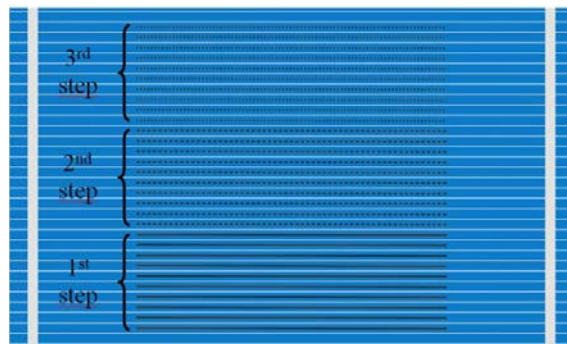


Figure 1: sketch of the experimental approach chosen for this work.

For illustration Figure 2 shows typical ablation lines on the surface of mc-Si solar cells. In the first micrograph the laser pulses are spatially separated, in the second a continuous line is created by overlapping pulses. In this work process parameters are selected so that the laser pulses along the ablation lines are separated. This eliminates the influence of pulse overlap.

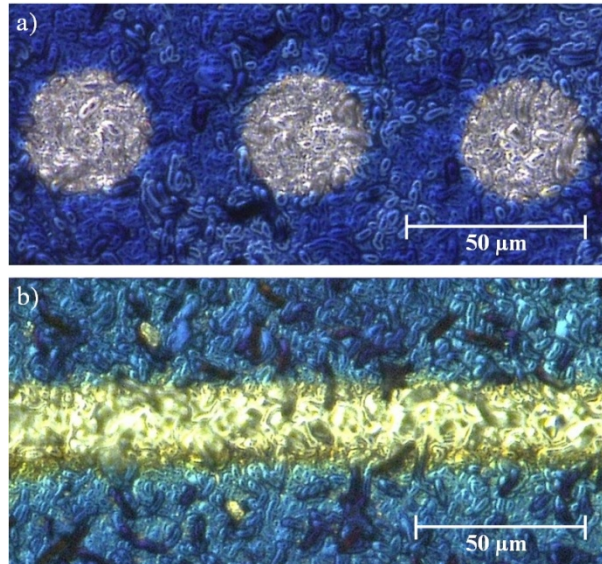


Figure 2: Micrographs of SiNx ablation with separated pulses (a) and with high overlap (b). Molten and re-solidified silicon is visible in the form of smoothed out surface texture in (b).

To allow a comparison of ablation results using different laser sources, the surface area opened per ablation step should be of the same order of magnitude for each set of parameters. This is achieved by adjusting the length of the ablated lines (between 30 and 80 mm) depending on the focus diameter.

Compared to other approaches presented in earlier works the method described above has two decisive advantages: a) there is no need to prepare special samples (e.g. full cells without front metallization) but commercially available standard solar cells can be used, enabling a reliable and easy characterization; b) due to the step by step ablation further information about the development of laser-induced damage during the process is obtained and the extrapolation to larger opened areas is possible.

2.2 Samples, characterization methods and reference cells

Standard 6 inch H-pattern multi-crystalline silicon (mc-Si) solar cells from the company Solland Solar Cells are used as samples. The thickness of the SiNx layer is about 80 nm. Note that these samples are already metallized and no processing step is taken out after laser ablation.

Characterization of the samples processed by laser ablation is taken out in a commercial Sinton Suns-Voc station. The measurement method illuminates the solar cell with a light flash and plots the voltage drop against the incident light power. In this way a pseudo I/V curve is obtained which neglects current and thus series resistance losses. The measurement mainly yields the open circuit voltage (V_{OC}) of the cell, but also provides several other properties by fitting a two diode model to the data. The fill factor derived from the measurement is termed pseudo fill factor (pFF), due to the neglect of current and ohmic losses. Details of the measurement can be found in [7, 8].

V_{OC} and pFF are determined before laser ablation (i.e. for the solar cell as it was provided by Solland Solar) and between the ablation steps. The study was taken out on 100 solar cells with an average V_{OC} of 608 ± 4 mV and an average pFF of $81.3 \pm 0.4\%$. Due to the comparison to the initial value, V_{OC} and pFF are considered sufficient characteristic values for this study. In the following, only relative values are used showing the deviation from the initial value.

In addition, a digital microscope is used to obtain micrographs of the ablated areas. The diameter of the ablated area per pulse ("spot size") is determined in this way.

Two different effects created by the ablation have to be considered: the damage to the emitter done by the laser irradiation and the opening of the irradiated area, which causes a reduction of passivation and increased surface reflectivity. To determine the influence of a loss of area covered by SiNx on the electrical cell properties a reference cell is created. Here, instead of using a laser source for SiNx removal, the layer is opened by wet chemical etching. Lines

with a width of about 1 mm are opened between the fingers. Two references are created in this way with a total opened area of 150 resp. 450 mm².

The characterization of the references showed no degradation of the electrical properties. This is inconsistent to the understanding of the beneficial effect of the passivation layer on the cell performance. Nonetheless, it is assumed that the degradation is minute and thus the dominating effect observed in this study is the laser-induced damage.

2.3 Experimental setup

Several different laser sources are used for the SiNx ablation to determine the influence of wavelength (355 and 532 nm), pulse duration (225 fs to 10 ps, 6 and 40 ns) and fluence (0.03-13 J/cm²). Table 1 summarizes the main parameters of the used laser sources.

The beam is moved across the sample by a galvanometric scanner. The scanner head is mounted to the z-axis of a 3-axis positioning system. The beam is focused by an f-theta lens with a focal length of 255 mm, which allows the processing of a full 6 inch solar cell without moving the positioning system.

The fluence (i.e. energy density on the sample) is defined by the amount of pulse energy per illuminated area (focal diameter at 1/e² of intensity). The focus diameter is measured by a beam profile camera. In this study the focus diameter is kept constant at around 45 μm.

Table 1: Laser sources used in this study

	Lightconversion "Pharos"	Trumpf "TruMicro 5250"	Newport Spectra- Physics "Explorer XP"	Lumera "Hyper Rapid 50"	JDSU "Q301"
Wavelength	532 nm			355 nm	
Pulse duration	0.2-10 ps	7 ps	6 ns	10 ps	40 ns
Average power	< 5 W	< 25 W	< 5 W	< 25 W	< 10 W
Repetition rate	< 600 kHz	< 400 kHz	< 300 kHz	< 1 MHz	10 kHz
Pulse energy	< 100 μJ	< 60 μJ	< 70 μJ	< 70 μJ	< 1 mJ

3. RESULTS

Figure 3 shows an excerpt of the data obtained by the experiments described above. The relative V_{OC} and pFF are plotted over the opened area for all laser sources under study. The fluence is fixed to 0.5 J/cm² here, except for the data obtained with 355 nm and nanosecond pulses, where a considerably higher fluence is required to achieve comparable spot sizes (4.4 J/cm²). This observation is discussed in section 4. The colors used in the graph denote the respective wavelength, while equal symbols correspond to equal pulse durations. This notation is used throughout the paper.

The left plot illustrates that the V_{OC} is only weakly influenced by the laser ablation (it varies between ±1% of the initial value) and no systematic dependence on process parameters is observed. However, as the right graph shows, the pFF degrades linearly with increased opened area and a distinct influence of pulse duration and wavelength can be seen. The pseudo fill factor is a measure of the quality of the cell's I/V characteristic. It can thus be utilized for an in-depth study of the laser-induced damage. To simplify the evaluation of the experimental data, in the following the slope of the pFF degradation (as visible in Figure 3 on the right) is utilized as the single value characterizing the laser-induced damage affecting the solar cell. This slope is named "pFF loss ratio" in the following.

The pFF loss ratio is given in 1/cm². For example a value of 0.01/cm² implies that the pFF is reduced by 1% (relative to the initial value) per opened cm². For a finger grid of 60 fingers with a width of 50 μm an area of 4.7 cm² needs to be opened. This shows that a useful laser ablation process needs to achieve loss ratio values around 0.002/cm² to keep pFF losses below 1%.

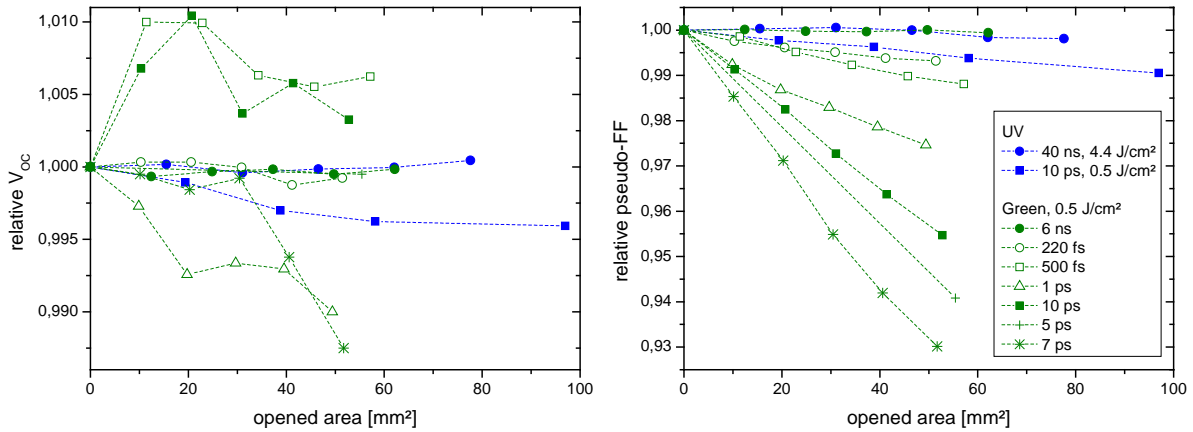


Figure 3: Relative values of open circuit voltage (V_{oc} , left) and pseudo fill factor (FF, right) plotted over the area of ablated SiNx. Lines are added to guide the eye. The symbols and colors in the plots are used throughout the paper to denote wavelength and pulse duration.

As will be discussed in section 4 pulse duration and wavelength both strongly influence the pFF loss ratio and thus the suitability of a certain laser source for the SiNx ablation process. The following sections show an in-depth analysis of the data obtained for this study, highlighting the influence of pulse duration and wavelength individually.

3.1 Influence of pulse duration

Two pulse duration regimes are included in the presented study: nanosecond pulses corresponding to the so-called short pulse regime as well as pico- and femtosecond pulses corresponding to the ultra-short pulse regime. It is commonly understood [9] that light-matter interaction in the short pulse regime is dominated by thermal effects and process results are characterized by melting and re-solidification of the material. In contrast, in the ultra-short pulse regime the pulse duration is shorter than the time required for thermalization of the energy, thus thermal effects occur less and less with lower pulse duration.

This effect is illustrated in Figure 4, where the ablation using 5 picoseconds (left) and 6 nanoseconds (right), respectively, at a wavelength of 532 nm is shown. In both cases the spot size is similar, which means the distance to the ablation threshold is similar (since the focus diameter is equal in both cases). The ablation with nanosecond pulses shows the characteristic smoothed out texture in the spot center (where the Gaussian energy distribution has its maximum), which is generated by melting and re-solidification of the Silicon during irradiation. As shown in Figure 2 this effect can also occur when using ultra-short pulse lasers, if the spot overlap is high or the ablation takes place far above threshold. In these cases thermal effects become dominant again.

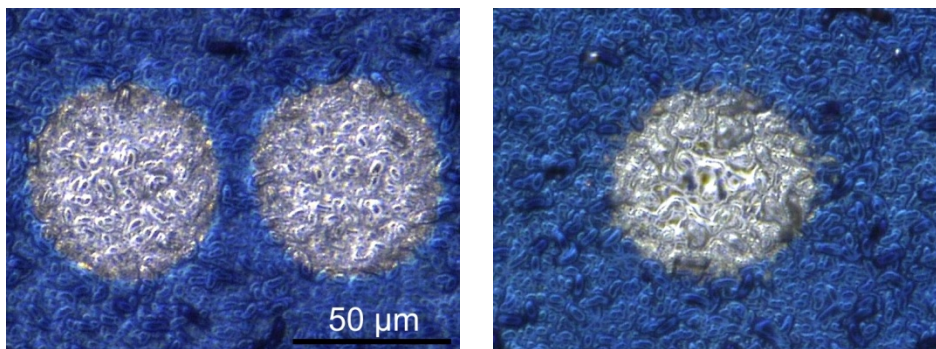


Figure 4: Micrographs of ablated spots created with 5 picosecond pulses (left) resp. 6 nanosecond pulses (right), both at 532 nm wavelength and similar fluence (1.5 J/cm^2). The center of the nanosecond ablation shows traces of molten and re-solidified silicon.

A direct comparison of the pFF loss ratio for short and ultra-short pulse ablation is shown in Figure 5. The wavelength is 532 nm. While the losses with nanosecond pulses are below the accuracy of the measurement method and oscillate

around 0 for low fluences, for 200 fs pulse duration a distinct dependence on fluence is visible. The curve shows a minimum value of the loss ratio at 0.3 J/cm², where the spot size on the sample is 40 μm.

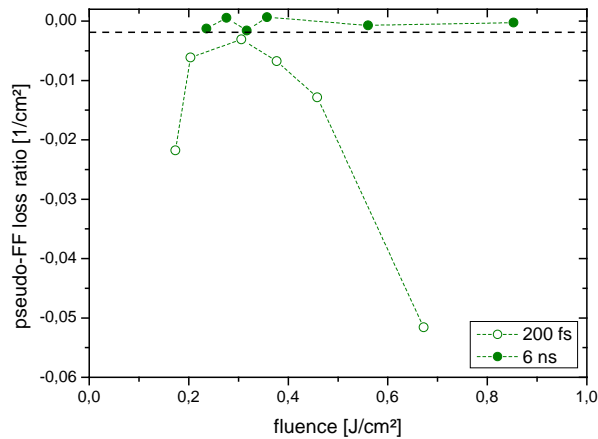


Figure 5: Comparison of the pFF loss ratio for ultra-short pulse and short pulse ablation. The values represent the best results found in this study.

Similar behavior is found for all experiments utilizing ultra-short pulse durations. Figure 6 summarizes the results for pulse durations between 200 fs and 10 ps. For all pulse durations in this graph the curves show a characteristic shape, which can in part be explained by the definition of the pFF loss ratio: for low fluences close to the ablation threshold the spot size and thus the total opened area decreases rapidly. Laser-induced damage can however also occur below threshold (e.g. by modifying the material due to thermal effects). This means the value of the loss ratio is dominated by the small value of the denominator. For high fluences far above threshold the laser-induced damage further increases with incident energy while the spot size (and thus the total opened area) remains more or less constant. For the ablation process the fluence range just above threshold is the most interesting (0.2 to 0.5 J/cm²). Here, all curves show a minimum in loss ratio. The spot size at this minimum is nearly equal for all pulse durations (40-50 μm).

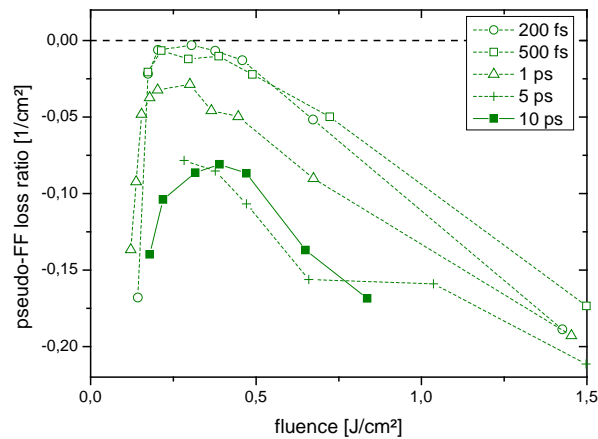


Figure 6: pFF loss ratio plotted over fluence for different pulse durations at 532 nm wavelength. The zero value of the loss ratio is indicated by the dashed line to improve readability of the graph.

Figure 6 shows that the pulse duration strongly influences the laser-induced damage. The minimum in pFF loss ratio is found at the lowest pulse duration (200 fs). Up to 5 ps the loss ratio increases, however it seems to reach a maximum at this point, since the data obtained at 10 ps shows no further increase. To investigate the reason for the improvement of the loss ratio with decreasing pulse duration, Figure 7 shows an example of the ablation at 200 fs (left micrograph) and at 5 ps (right) pulse duration. No distinct differences are visible, which can be expected: the emitter layer, which in large part determines the electrical properties of the solar cell, is only 300 nm thick. An ablation or other laser-induced damage inside such a thin layer is invisible for standard optical microscopy.

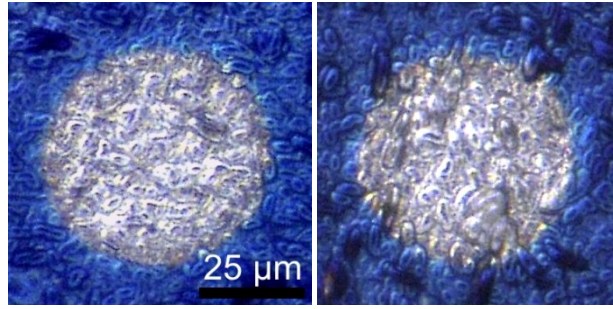


Figure 7: Comparison of ablation spots created with 200 fs (left, 0.7 J/cm²) and 5 ps (right, 0.5 J/cm²) pulse duration (at 532 nm wavelength).

3.2 Influence of wavelength

The wavelength of the laser radiation directly determines the absorption resp. penetration depth in the material. The two wavelengths included in this work are 355 nm and 532 nm. The respective penetration depths into Silicon are 10 nm and 1.2 μm [10]. Since the emitter layer is only 300 nm thick, the proper selection of the wavelength is critical for the ablation process.

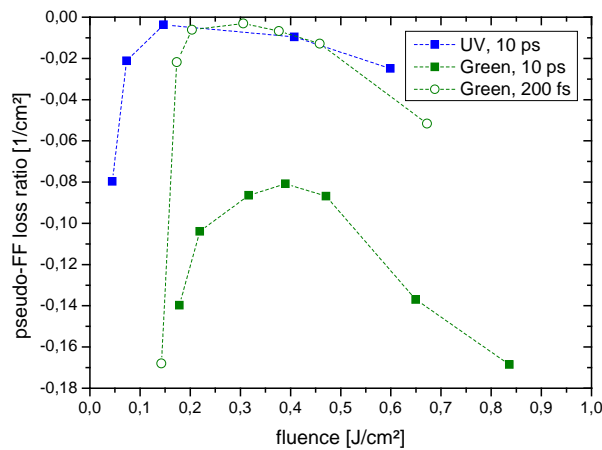


Figure 8: pFF loss ratio plotted over fluence for ablation using picosecond pulses at 355 and 532nm wavelength.

Figure 8 and Figure 9 show the development of the pFF loss ratio with fluence. In Figure 8 the effects of ultra-short pulses on the loss ratio are shown. For two curves (square symbols) the same pulse duration of 10 ps was chosen for direct comparison. The loss ratio is one order of magnitude smaller at 355 nm wavelength. The curve for 200 fs pulse duration shows that the minimum loss ratio is nearly equal at 200 fs, 532 nm and 10 ps, 355 nm.

Figure 9 shows a similar comparison for the short pulse regime. On the left, the loss ratio is again plotted over fluence. However, as described above, the fluences required for SiNx ablation are considerably higher at 355 nm wavelength at nanosecond pulse durations. Thus, on the right the loss ratio is plotted over the spot size to show that the ablation process results in similar SiNx openings in the range of 40 μm. However, no systematic dependence on fluence or spot size is found, probably since the loss ratio values are within the error margins in this case. In summary, the graphs show that the laser-induced damage is very low in the nanosecond regime and that the loss ratio is in general lower for a wavelength of 532 nm.

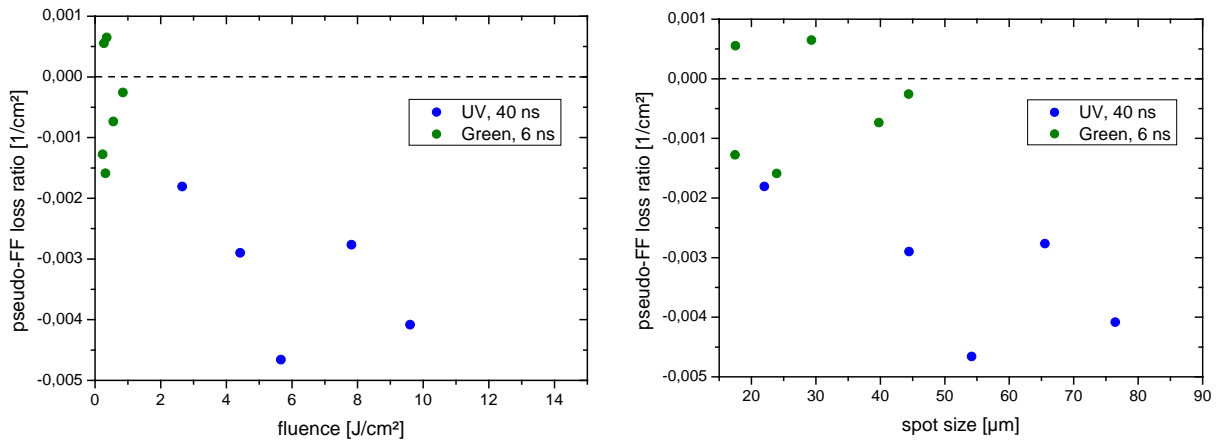


Figure 9: pFF loss ratio plotted over fluence (left) and spot size (right) for ablation using nanosecond pulses at 355 and 532nm wavelength. The right plot illustrates that the ablated areas per pulse are of similar size for both wavelength, while the fluences required for this ablation are lower by one order of magnitude for 532nm wavelength.

For a visual comparison Figure 10 shows micrographs of the SiNx ablation utilizing nanosecond pulses at 532 (left) and 355 nm wavelength (right). The color difference in the images is due to different microscope settings. Still, a significant difference is visible in the images: at 532 nm the ablation is circular and the edge of the spot is rather homogeneous. At 355 nm the edge is very inhomogeneous and darker regions within the spot are visible, where the SiNx was not or not fully ablated. These regions correspond to deep pits in the surface texture. If this observation is connected to the behavior found in the pFF loss ratio and why it occurs is not clear at this point.

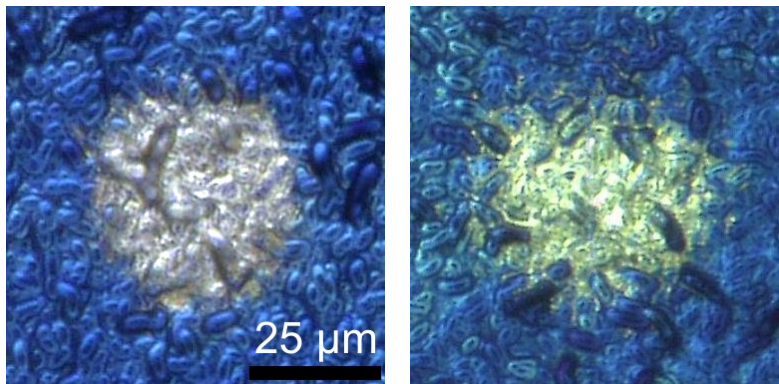


Figure 10: Comparison of ablation spots created with nanosecond pulses at 532 nm (left, 0.6 J/cm²) and 355 nm (right, 4.4 J/cm²) wavelength.

4. DISCUSSION

Figure 6 shows that pulse durations in the femtosecond regime result in very low pFF loss ratio values. With increasing pulse duration the values increase. The data indicates a maximum at around 5 ps pulse duration, but the data base needs to be expanded to strengthen this argument. However, such an effect can be expected: the energy absorption and distribution effects are determined by electron-electron, electron-phonon and phonon-phonon interactions. The fastest process, the electron-electron interaction, occurs in a time domain around 100 fs. The electron-phonon interaction is dominant in a time domain around 10 ps. Only after 50-100 ps the phonon-phonon interaction (the thermalization of the energy into the solid state body) takes place. The transition between a dominant electron-electron and a dominant electron-phonon interaction occurs at around 1 ps. These time domains strongly depend on the material properties and can only be used as rough estimates. However, this argument supports the experimental evidence that the laser-induced damage is strongest for pulse durations between 1 and 10 ps: for lower pulse durations so-called “cold” ablation (ablation without thermal effects) can take place, which is dominated by sublimation of the material. For higher pulse durations

thermal effects lead to melting. This can result in very low pFF loss ratio values as the experiments with nanosecond pulse durations show.

The low degradation of the electrical properties of solar cells for laser ablation in the nanosecond pulse duration regime was observed in earlier works as well [3]. The melting of the Silicon can lead to a drive-in effect of the Phosphor atoms which are used for emitter doping. The result is comparable to the effect of the laser doping process, which not only introduces additional atoms into the emitter region, but also creates a deeper emitter. However, if this effect is beneficial or undesirable for a combination of laser ablation and subsequent metallization needs to be clarified.

In the comparison of ablation results using 532 nm and 355 nm radiation it was found that for pulse durations of 10 picoseconds lower pFF loss ratio values are obtained with 355 nm. On the other hand, with nanosecond pulses the loss ratios obtained with 532 nm wavelength were lower. In both cases this can be explained by the difference in penetration depth: at 355 nm wavelength the penetration depth is only 10 nm, lower than the SiNx layer thickness of about 80 nm and the emitter thickness of about 300 nm. For picosecond pulses this means that the laser-induced damage only occurs in depths lower than the emitter thickness and the effects on the electrical properties of the cell are lower. For 532 nm the penetration depth is of the order of 1 μm , much larger than the emitter thickness. Here, the laser-induced damage can reach deeper into the emitter leading to stronger material degradation.

For nanosecond pulses the opposite is the case: at 532 nm wavelength the energy can dissipate to heat deeper in the material and can thus lead to stronger emitter drive-in. If this argument is true has to be investigated more closely, e.g. by characterization of the emitter profiles after ablation. However, it is in line with other works on laser doping, where the clear choice is a wavelength of 532 nm, since with 355 nm lower conversion efficiencies are obtained [11, 12].

As observed in the beginning of section 3 the ablation process at a wavelength of 355 nm and with nanosecond pulse duration requires considerably higher fluences. This is also in line with the argument above, since at a penetration depth of only 10 nanometers the thermally driven ablation process requires more energy to remove the 80 nm thick SiNx layer than the ablation at 532 nm.

The lowest pFF loss ratios obtained in this study (with a spot size of 40 μm for comparability) are summarized in Table 2.

Table 2: Process parameters of the best pFF loss ratio values obtained in this study.

wavelength [nm]	pulse duration [ps]	fluence [J/cm ²]	pFF slope [1/cm ²]
355	10	0,2	-0,004
355	40000	4,4	-0,003
532	0,2	0,3	-0,003
532	6000	0,9	-0,0003

5. CONCLUSIONS

This work describes an in-depth study of the influence of pulse duration and wavelength on the electrical properties of multi-crystalline solar cells which were processed by pulsed laser ablation of Silicon Nitride passivation layers. Full commercial solar cells were used as test vessels. The study focusses on the evaluation of the degradation of the pseudo fill factor (pFF). A distinct influence of the pulse duration in the range between 200 fs and 10 picoseconds was observed. While the laser-induced degradation strongly increases with pulse duration this trend seems to reverse beyond 5 ps.

Two wavelengths were included in the study: 355 nm and 532 nm. In the nanosecond pulse regime effects similar to those reported from laser doping studies can be observed. The melt-driven ablation process at these pulse durations yields lower cell degradation for 532 nm wavelength. This can be attributed to an emitter drive-in effect, which occurs during the ablation within the Silicon. At 355 nm wavelength the short penetration depth (about 10 nm) leads to a weaker emitter drive-in than at 532 nm wavelength.

For ultra-short pulses the wavelength has the opposite effect: here, 355 nm radiation creates less laser-induced degradation, probably because emitter degradation is limited to a depth of a few ten nanometers.

Very low degradation of electrical properties after ablation is achieved with ten picoseconds and 40 nanoseconds at 355 nm as well as 200 fs at 532 nm. Here, the pFF is reduced by about 0.3%_{rel} per cm² of opened area. For a metallization grid of 60 fingers with a width of 50 μm an area of 4.7 cm² needs to be ablated. The pFF would be reduced by about 1.1 to 1.4%_{abs}. This is probably too high for a functional industrial ablation process.

The best results were obtained with 6 nanosecond pulses at 532 nm. Here, the relative loss of pFF is 0.003% per cm². For a full cell this would amount to only 0.1% absolute loss in pseudo fill factor. The authors assume that such a result is sufficient for an industrial implementation of the ablation process. However, it is not known at this point, if the emitter drive-in effect occurring for ablation with nanosecond pulses is beneficial for a combination of laser ablation and subsequent metallization.

This study did not cover the effects of spatially overlapping laser pulses. Since pulse overlap can lead to increased thermalization of the pulse energy this could be especially interesting for ultra-short pulses. In the future a transfer of the results of this study into the pilot production of solar cells is required to ascertain that the results obtained here are also valid when a metallization process is applied to the ablated areas.

6. ACKNOWLEDGEMENTS

The work was supported by the European Union within the project "Solasy - Next Generation Solar Cell and Module Laser Processing System"; EU Grant No. 21905. The authors would like to thank the project partners for support, discussion and feedback and Jo Das (formerly at IMEC) for preparation of the reference cell.

REFERENCES

- [1] Moritz Schaefer, Malte Schulz-Ruhtenberg, Jens Holtkamp, and Arnold Gillner. Comparison of laser ablation of transparent conductive materials on flexible and rigid substrates. In *Proceedings of LOPE-C 2012*, 2012.
- [2] M. Hoerteis and S.W. Glunz. Short communication: Accelerated publication fine line printed silicon solar cells exceeding 20% efficiency. *Progress in Photovoltaics: Research and Applications*, 16(7):555–560, 2008.
- [3] J.L. Hernandez, C. Allebe, L. Tous, J. John, and J. Poortmans. Laser ablation and contact formation for cupulated large area c-silicon industrial solar cells. In *Proceedings of 35th IEEE Photovoltaic Specialist Conference*, 2010.
- [4] Thorsten Dullweber, Sebastian Gatz, Helge Hannebauer, Tom Falcon, Rene Hesse, Jan Schmidt, and Rolf Brendel. Towards 20% efficient large-area screen-printed rear-passivated silicon solar cells. *Progress in Photovoltaics: Research and Applications*, doi: 10.1002/pip.1198, 2011.
- [5] Matthieu Moors, Kasper Baert, Tom Caremans, Filip Duerinckx, Antonio Cacciato, and Jozef Szlufcik. Industrial perl-type solar cells exceeding 19% with screen-printed contacts and homogeneous emitter. *Solar Energy Materials and Solar Cells*, doi: 10.1016/j.solmat.2012.05.006, 2012.
- [6] Annerose Knorz, Marius Peters, Andreas Grohe, Christian Harmel, and Ralf Preu. Selective laser ablation of SiN_x layers on textured surfaces for low temperature front side metallizations. *Prog. Photovolt: Res. Appl.*, 17(2):127–136, 2009.
- [7] R. A. Sinton. Possibilities for process-control monitoring of electronic material properties during solar cell manufacture. In *NREL 9th Workshop on Crystalline Silicon Solar Cells and Materials and Processes*, 1999.
- [8] S. Bowden and A. Rohatgi. Rapid and accurate determination of series resistance and fill factor losses in industrial silicon solar cells. In *Proceedings of 17th European Photovoltaic Solar Energy Conference*, pages 1802–1806, 2001.
- [9] John Dowden, editor. *The Theory of Laser Materials Processing*. Springer, 2009.

- [10] M.A. Green and M. Keevers. Optical properties of intrinsic silicon at 300 k. *Progress in Photovoltaics: Research and Applications*, 3:189–192, 1995.
- [11] M.C. Morilla, R. Russell, and J.M. Fernandez. Laser induced ablation and doping processes on high efficiency silicon solar cells. In *23rd European Photovoltaic Solar Energy Conference*, 2008.
- [12] J.M. Bovatsek, A. Sugianto, B. Hallam, B. Tjahjono, S.R. Wenham, and R.S. Patel. High-speed fabrication of laser doping selective emitter solar cells using 532nm continuous wave (cw) and modelocked quasi-cw laser sources. In *Proceedings of 26th European Photovoltaic Solar Energy Conference*, 2011.